Magazine of Civil Engineering. 2019. 85(1). Pp. 136–145
Инженерно-строительный журнал. 2019. № 1(85). С. 136–145

Magazine of Civil Engineering

ISSN 2071-0305

journal homepage: http://engstroy.spbstu.ru/

DOI: 10.18720/MCE.85.11

Structural health monitoring of a concrete-filled tube column

A. Younesi[a], O. Rezaifar[a]*, M. Gholhaki[a], A. Esfandiari[b],
[a]Semnan University, Semnan, Iran
[b]AmirKabir University, Tehran, Iran
** E-mail: orezayfar@semnan.ac.ir*

Keywords: CFT column; modal data; damage identification; Structural Health Monitoring; CWT.

Abstract. Structural Health Monitoring (SHM) has provided an opportunity to assess the reliability and integrity of civil engineering structures. Damage in the structure reduces the hardness and modal properties of the structures. Therefore, changes in dynamic behavior and modal data can be used to identify damage. This study identifies the existence and location of damage in the CFT column based on vibrational analysis techniques. The method for damage detection is based on dynamic analysis on the modal data (mode shape, frequency and damping) of the structure. The experimental results obtained the modal test and the results of the theory of FE simulation have been used to identify the damage. In the first step, after creating the prototype and preparing the test setup, the specimen was subjected to a modal test, so the modal data were extracted, and the Coherence curve test were plotted to confirm the accuracy. Similarly, the FE model is also simulated after validation, so the modal data of the theory were also extracted. In the second step, based on the obtained data, the comparison of frequencies, MAC and COMAC criteria, mode shape and damping of an undamaged and damaged specimens were performed, and the identification of the damage was dealt with. In the third step, the Continuous Wavelet Transform(CWT) tool was used in order to determine the location of the damage in both methods (FE and experimentally), to identify the damage location on the mode shape (CWT input signal). The results show that in the both the methods, the existence of damage in the CFT column is well identified and its location is also determined with high precision, which indicates the ability of damage detection method by CWT techniques.

1. Introduction

CFT columns are very important because of their widespread use in high-rise buildings. On the other hand, due to the combination of two materials with a distinct mechanical behavior, the possibility of the occurrence of malfunction and damage under load is high. Identifying damage in this highly applied structural element is very important. Accordingly, the number of researches done on the identification and localization of the estimation of the health status of CFT columns is increasing, which is due to: 1. Executive weakness, 2. Thinness of plates and their buckling probability, 3. Extensive application, 4. High age of structure, and 5. Lack of proper connection between concrete and steel. In the present study, the detection of damage to the CFT column under the plate local buckling damage (shrinkage of the plate under pressure) has been carried out, where to simulate a part of the column is cut in parallel grooves to indicate the buckling damage. In addition, laboratory modal data and extracted theory and modal analysis have been carried out on them to identify the presence of damage and its exact location.

Most damage detection methods are based on data obtained from the Fourier transform spectra. Damage to structures is usually local, which can usually be identified by identifying Mode shapes. [1–3].

The study of A. Lyapina and Y. Shatilov Investigates the identification of the position of damage in concrete columns using vibration analysis techniques. The method for detecting and locating damage is based on the analysis of the dynamic characteristics of a structure, such as Eigen-frequencies, mode shapes and modal damping. The results of the FE analysis show that increasing the number of sensors increases the accuracy of the location of the damage [4]. A theoretical and experimental study of the frequency-based

Younesi, A., Rezaifar, O., Gholhaki, M., Esfandiari, A. Structural health monitoring of a concrete-filled tube column. Magazine of Civil Engineering. 2019. 85(1). Pp. 136–145. DOI: 10.18720/MCE.85.11.

damage detection method has been presented in Chen Yang and S. Olutunde Oyadiji. Based on the eigenvalue problem and perturbation assumption of defect in modal response, the theoretical basis of the modal frequency curve method is established. The numerical and experimental results show that the damage indicator is more accurately detected than the wavelet coefficients. Additionally, the damage estimator shows the size of damages with high precision [5]. A number of researchers have examined the effects of frequency changes on damaged structures compared to healthy structures. [6–9]. In addition, Gadelrab studied the frequency change due to damage on a two-layer beam. The results showed that frequency changes depend on boundary conditions [10]. Results of studies Kessler et al. [11] showed that the reduction of frequency in low modes is proportional to the reduction of general stiffness. Della and Shu investigated several numerical modeling techniques of damage detection. The results indicate that natural frequency changes detect the position and size of the damage [12]. Alnefaie [13] showed that the defect-induced variation of mode shape is more distinct for higher flexural vibration modes. Salawu has reviewed various agencies. This study shows the possibility of using modal frequency data in identifying damage and structural health monitoring [14]. Comprehensive studies of structural health monitoring methods based on vibrational methods have been reported [15]. Although the natural frequencies of the structure can be accurately measured with a number of sensors, but modal frequency changes cannot be detected the location of the damage [16, 17]. In recent years, the CWT method has been considered for further damage identification. Hong et al. investigated damage detection based on Mexican hat wavelet coefficients using CWT and Discrete Wavelet Transform (DWT). They suggested that the number of vanishing moments of wavelets in crack detection should be at least two [18, 19]. Chang and Chen used the DWT to obtain Gabor wavelet transform coefficients for crack detection and localization in the beam [20].

The damage is estimated based on the specified parameters of the criterion and the damage summation procedure by employing the FE method. With a reasonably fine mesh of the FE model of the “critical location” structure, the condition of the identity of damage in the material of the test specimen and the structure is provided and, respectively, the effect of uncertainty on the fatigue life assessment of the structure is reduced. The implementation of this version of the method is using the example of the fatigue life evaluation of a ship hull and superstructure detail at expansion joint. For comparison, the fatigue life of the detail is estimated using the standard S-N approach. The results are in approximate agreement; however, reducing the computational uncertainties with the help of the deformation criterion shows more physically reasonable fatigue properties of the detail [21–23].

Due to the defects in the connections and the force transfer from the beam flanges to the column of the hollow section and concrete filled tube steel columns, different types of internal and external stiffeners have been suggested. By installing external stiffeners, the implementation problems of the construction of the columns and the internal hardening of the installation is minimized [23–28].

The paper reviews the recent applications of piezoelectric materials in structural health monitoring and repair conducted by the authors. First, commonly used piezoelectric materials in structural health monitoring and structure repair are introduced. The analysis of plain piezoelectric sensors and actuators and interdigital transducer and their applications in beam, plate and pipe structures for damage detection are reviewed in detail. Second, an overview is presented on the recent advances in the applications of piezoelectric materials in structural repair. In addition, the basic principle and the current development of the technique are examined [29]. The identification of the segregation of steel tube from the central core in the rectangular CFT column has been evaluated based on the energy spectrum of the CWT with the piezo ceramics [30–32]; the segregation of core enclosed from the steel tube reduces bearing capacity and structural shape ability. In the study of Xu, B. et al., with the installation of piezoelectric in predetermined locations on the external surfaces as a sensor, a new method is proposed to monitor the interior state. In this study, wavelet energy spectrum analysis was also performed and a weight-based damage index (WPES) was defined for the determination of artificial segregation regions. The results show that the proposed indices are sensitive to segregation defects and fully assess the internal surface of a CFT column. In addition, the results show that there can be no undetectable segregation defects in the monitoring of the health of CFT column in high-rise structures.

Since the damage of shrinkage of steel tube plate in CFT column, because of its thinness – due to its high ratio of strength to steel weight – is one of the most noticeable damages occurring to this structural element, it is evaluated in this study. In order to simulate damage, the damage location is cut in parallel grooves. Also, in order to reveal damage in steel columns filled with concrete, laboratory modal analysis was used. After the modal data were extracted, the process of the presence of damage was detected by comparing frequencies, mode shape and parameters of MAC and COMAC, and a one-dimensional CWT method has been used to determine the exact location of the damage.

2. Methods

2.1. Test Specimens

Two specimens of CFT columns with similar characteristics were used to perform the test that an intentional damage has been created in the wall of one of the specimens. The column section of the specimens is 120*120mm from the steel plate with a thickness of 3mm and a length of 800mm which is filled with fine aggregate concrete. In order to simulate damage a Parallel groove (thickness of grooves are 2.5mm) with the size of 114*45mm with similar thickness of the plate has been created in the middle of one of the column, which indicates the local buckling in the column plate. The specimen specification has been presented in Table 1 and Figure1.

Table 1. Introduction of Specimens.

Specimen	Damage dimension(mm)	Damage type	Damage location
UDS-P	-	Healthy	-
DLB-P	114 * 45	Column plate buckling	Middle of the column

It is worth noting that the damage was created by the high precision before filling the column and the site of damage is completely filled in order to prevent the release of the concrete. After the concrete has reached the strength required, the filler material has been removed from the site of damage (see Figure 1).

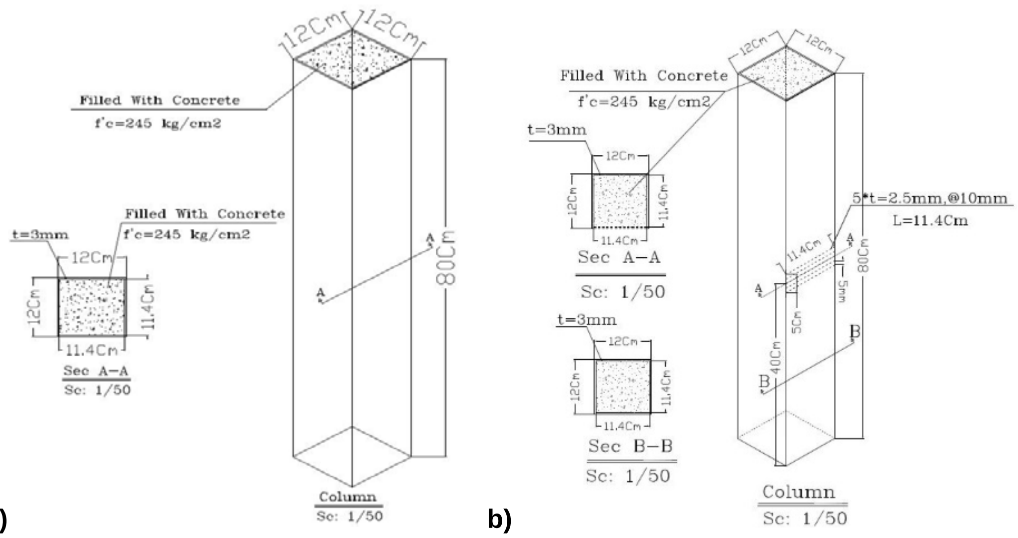

a) b)

Figure 1. Test specimens; (a) UDS-P, (b) DLB-P.

2.2. FE models

ABAQUS limited component software was used for modeling specimens. Solid and Sell elements were used for modeling concrete and steel plates. At the point of concrete contact with steel, the coefficient of friction is 0.7. The final models are shown in Figure 2.

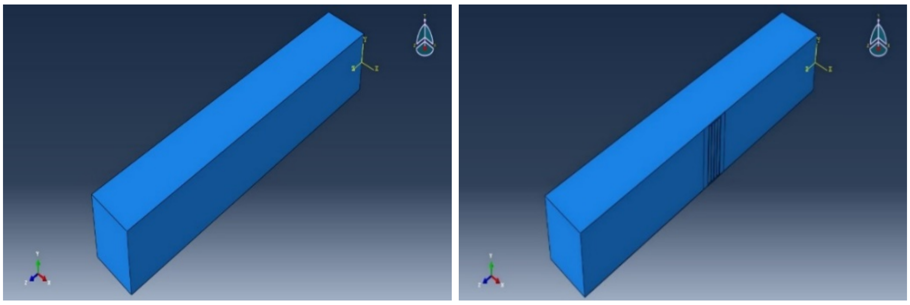

a) UDSP **b) DLBP**

Figure 2. FEmodels.

2.3. Material Properties

The main materials used in this study were steel and concrete. The steel used was of type st37, the characteristics of which after the tensile test are presented in Table 2. The concrete used was composed of the fine grain materials, the mechanical properties of which after the compressive test on cubic specimens are presented in Table 2.

Table 2. Material properties.

Materials	$f_y(MPa)$	$f_u(MPa)$	$f'_c(MPa)$	$E(MPa)$	ϑ	Specific gravity ($\frac{kN}{m^3}$)
Steel	327.26	391.12	-	2.00×10^5	0.29	78.50
Concrete	-	-	26.06	0.79×10^5	0.20	24.40

2.4. Test setup and instrumentation

Since the existence of any supporting conditions causes a high rigidity in the structure and a large force is required to stimulate it for modal analysis. This force may cause unforeseen damage and even damage of the structure and error in the results of the analysis. Therefore, the free-free support conditions have been used in the present study. To achieve this goal, the CFT column was suspended by an elastic ribbon with high elasticity (or on a low inflation tube) and the accelerometer was connected to it at a point in the column. (Figures.3 and 4). The location of connection of the accelerometer sensor has been selected between the midpoint and the edge of the beam so that firstly, not to be detached when an impact is applied, and secondly, to be placed at zero-moment point in order to be with the least error. In the next step, a force was applied to the stimulation points (the site of the mesh nodes) by a stimulus (stimulator hammer or shaker) and the frequency response function was extracted for each excitation. Finally, using the sum of the resulting frequency functions, the first to third modes of the frequency response function have been obtained in two different methods as follows.

The frequency response functions were obtained in two different ways: 1) Stimulation using a hammer: In this method, the specimen was placed on a tube. The sensor was then fixed at a specific location and stimulated by the impact hammer in different locations. It is important to note that the location of the sensor should not be placed on the node of the mode shape, which is why the point between the end and midpoint of the column was chosen as the location of the sensor installation. 2) Stimulation using a shaker: In this approach, the specimen was suspended using an elastic band. The shaker was fixed at a specific location on the specimen and the sensor was replaced in different places. Here it is also important that the shaker not to be located in the node. The random type of stimulus signal was selected to interpolate nonlinear effects of the specimen and provide the best linear model. Choosing the best type of stimulation depends on the geometry and structure of the specimen. For most of the specimens due to their non-linear nature, the hammer stimulation was not suitable and therefore, the shaker stimulation was applied. Finding the best method does not follow a general rule and is achieved with trial and error (Figures 3 and 4).

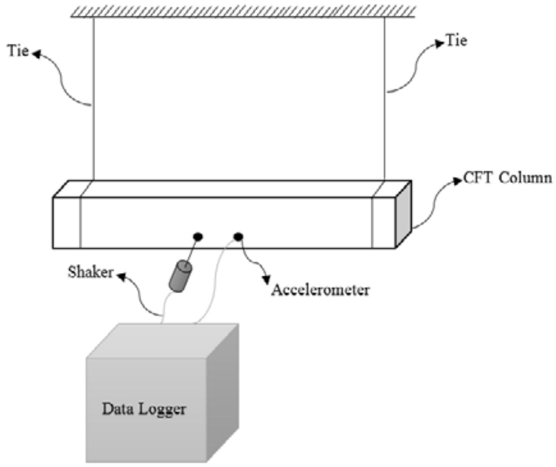

Figure 3. Test setup.

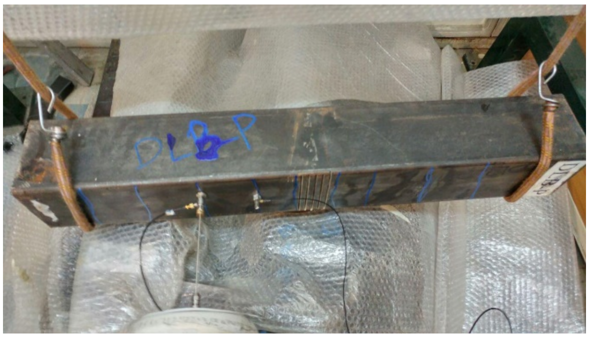

Figure 4. Tooling and testing method.

Table 3. The tools of tests.

No.	Equipment	Model	Manufacturer	Country of origin
1	PorTable Pulse 4/2 I/O Module	3560C	B&K	Denmark
2	Impulse Hammer	AU02	AP Tech	Netherland
3	Accelerometer	4397	B&K	Denmark
4	Charge Convertor	2646	B&K	Denmark
5	Force Transducer	9301B	Kistler	Switzerland
6	Power Amplifier	BAA120	Tira	Germany

3. Results and Discussion

3.1. General Observation of Experimental Tests

After the specimens are made and the structure is installed in the setup and the sensor is installed, the specimens are subjected to the shaker which shows how the specimens are tested in Figure4 then, the frequency, mode shape and damping patterns of the specimens have been extracted as modal data.

The specimen frequency in all modes is reduced compared to the healthy state which indicates the change in the mechanical characteristics and, consequently, the change in the dynamic behavior of the structure. In the monitoring of the health of the structures, frequency variation can be considered as an example of damage in the specimen. On the other hand, the damping coefficient in the DLB-P specimen has been increased in proportion to the healthy specimen (UDS-P). This is due to the hardening of the damaged specimen.

By observing the shape of the specimen mode, it is concluded that the amplitude of the mode in the damaged specimen is higher than the normal specimen and the structure has a softer behavior. It can also be concluded that the point-to-point slope of the mode shape in the specimen after damage is lower, which in general indicates a reduction in the stiffness of the structure. To determine the frequencies of each curve mode, FRF of the specimens have been extracted (Figure 5). On the other hand, COHERENCE curve has been plotted to monitor the accuracy of the tests. As the points in the COHERENCE curve are closer to one, it indicates the high accuracy of the experiments (Figure 6).

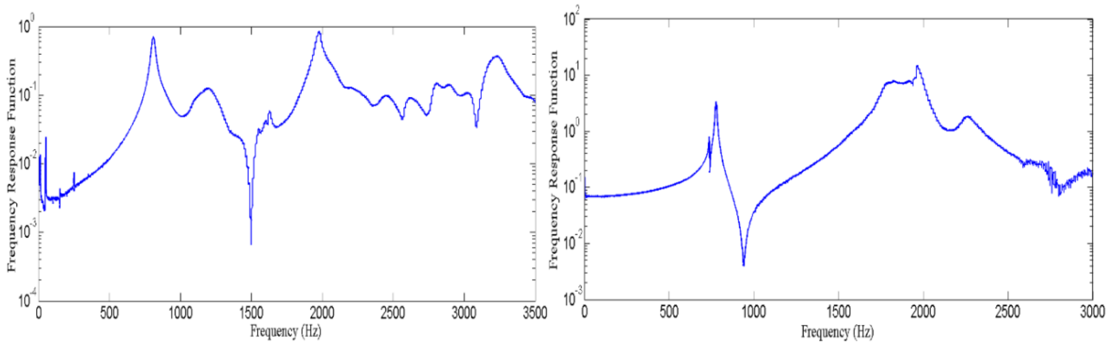

(a) UDS-P **(b) DLB-P**

Figure 5. Phase-Amplitude curve of the specimens.

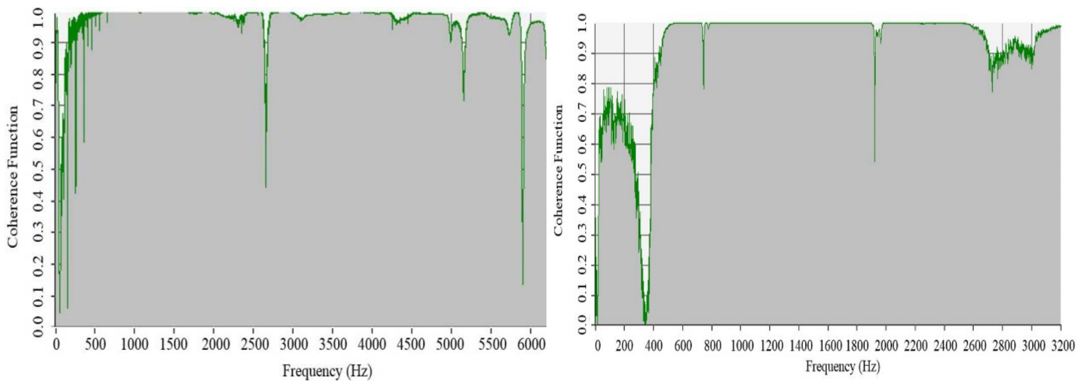

(a) UDS-P **(b) DLB-P**

Figure 6. COHERENCE curve of the specimens.

3.2. Mode Shape

Figures 7a to 7c shows the mode shape of both a normal and damaged specimen based on theoretical and laboratory data. As shown in Figure 7a, mode shape of the damaged specimens are further elongated in the damaged region (mid-column at 5 cm of length), indicating that changes are made in the mechanical properties. In addition, similar results have been achieved in models created in ABAQUS software. Similarly, in the second and third modes, both theoretical and experimental modes of simulated damage in the DLBP specimen have caused the shape of the mode to change from its normal mode (UDSP), which generally indicates the presence of damage in the structure.

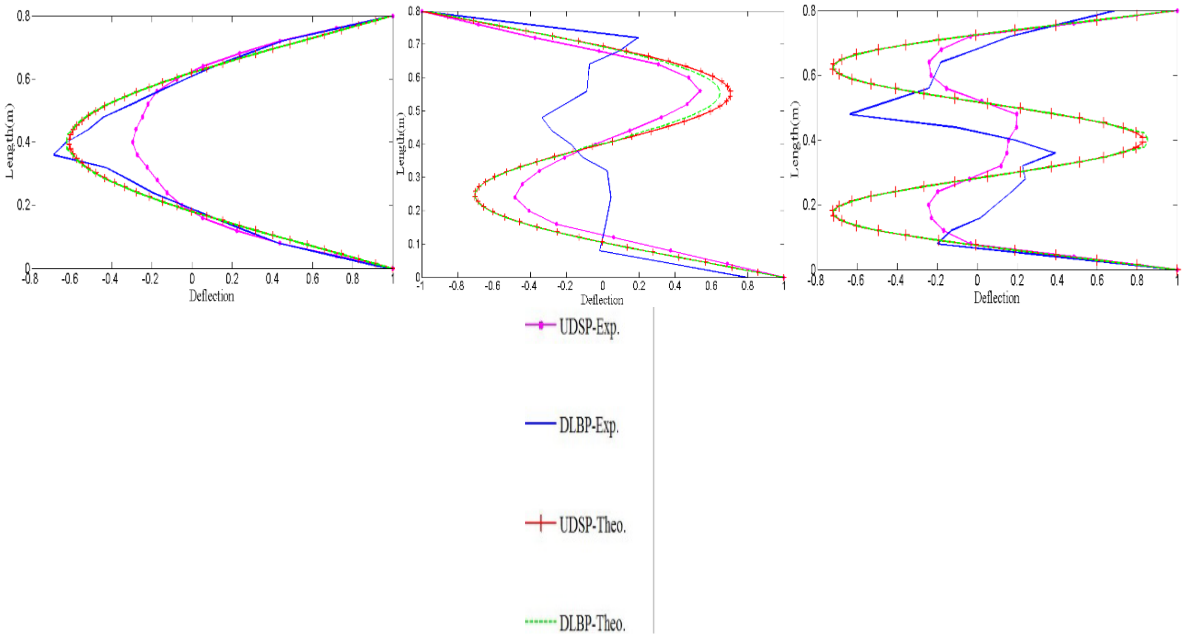

a) Mode I b) Mode II c) Mode III

Figure 7. Mode shapes of experimental specimens and Theoretical models.

3.3. Frequency

Another parameter for damage detection in structures is to compare the frequencies of damaged and normal specimens. In real structures, having a database of structures, you can continually monitor the health of the structure. In the present study, a normal specimen was first made and based on the mechanical properties obtained, the damaged specimen was made completely similar and only with a predetermined damage.

Table 4. Frequency of experimental specimens and theoretical models.

Type of test	Mode No.	Health	Damaged	Difference(%)
Experimental	Mode I	808.40	777.09	-3.87
	Mode II	1971.50	1962.40	-0.46
	Mode III	3218.90	2257.30	-29.87
Theoretical	Mode I	874.29	872.21	-0.24
	Mode II	2138.10	2135.80	-0.11
	Mode III	3686.80	3663.40	-0.63

According to Table 4, the frequency in the damaged specimen decreases in both theoretical and laboratory conditions, which indicates a change in the mechanical properties of the specimen, followed by a change in the modal parameters (frequency and model shape). The results show that the frequency change in the third mode is higher than other modes, so identifying damage at higher modes is easier and since achieving higher modes is difficult and requires more spending and may even cause serious damage to the specimen, frequency change in theoretical mode is less than that of laboratory whose reason is the more even simulation of materials and the connection between concrete and steel.

3.4. MAC and COMAC Parameters

One of the valid criteria for examining the damage in structures is the Modal Assurance Criteria (MAC) and Coordinate Modal Assurance Criterion (COMAC) [33].

$$MAC_{(j,k)} = \frac{\left(\sum_{i=1}^{n} \Phi_{Aj}^{i} \times \Phi_{Bk}^{i}\right)^2}{\sum_{i=1}^{n} (\Phi_{Aj}^{i})^2 \times \sum_{i=1}^{n} (\Phi_{Bk}^{i})^2} \qquad With: \quad j = 1,...,m_A \quad and \quad k = 1,...,m_B \qquad (1)$$

where: Φ_A and Φ_B are two series of mode shape expressed in matrix from, respectively of $n \times m_A$ and $n \times m_B$ class, with m_A and m_B equal to the number of investigated modes and n equal to the number of considered coordinates; Φ_{Aj}^{i} is the ith coordinate of the jth column of Φ_A, while Φ_{Bk}^{i} is ith coordinate of the kth column of Φ_B.

As MAC index does not take into account local deviations of displacement, it has been introduced another index, the COMAC, expressed the following [34]:

$$COMAC_{(i)} = \frac{\left(\sum_{k=j=1}^{L} \Phi_{Aj}^{i} \times \Phi_{Bk}^{i} \right)^2}{\sum_{j=1}^{L} (\Phi_{Aj}^{i})^2 \times \sum_{k=1}^{L} (\Phi_{Bk}^{i})^2} \quad (2)$$

Where L is the total number of investigated modes and i = 1…n is the generic point of measure. This index can be used to identify the positions in which the two series Φ_A and Φ_B of mode shape are discordant, because it measures the correlation between all the displacements at i`th point corresponding to the different modes. The value of one indicates the integrity of the structure and values less than one representing the probability of damage in the structure [34].

These criteria, by examining and comparing the modes of healthy and damaged specimens according to Eq. 1 and 2, investigate the presence of damage in these structures; the closer this value to one, the more the overlap of the modes under investigation, such that the number 1 represents the complete coincidence of the mode shapes (vectors) and the zero number represents the perpendicularity of these vectors (Table 5).

Table 5. Parameters of MAC and COMAC.

Theoretical		Experimental		Specimen	
DDB-P	UDS-P	DLB-P	UDS-P		
0.99993	1	0.92150	1	MAC	Mode1
0.99990	1	0.92150	1	COMAC	
0.99819	1	0.30390	1	MAC	Mode2
0.9982	1	0.71640	1	COMAC	
0.99972	1	0.46050	1	MAC	Mode3
0.99970	1	0.76350	1	COMAC	

One of the ways of detecting the presence of damage in structures is examining MAC and COMAC criteria. The more these values are less than one, indicates a greater change of the interested mode in the normal structure than damaged structure (the value of 1 indicates the complete conformation of the mode shape of the normal and damaged structure). Based on Table 5 and Figure 8, the values of MAC and COMAC in both laboratory and theory modes are reduced. In theory, the reduction of values is less than the experimental one. So that in the second mode, the MAC value is about 30 %, which indicates a very low conformation of the normal and damaged structures. In addition, the COMAC of this mode is also smaller than other modes. Generally, given the change of MAC values, it could be concluded that a damaged is occurred to the structure whose severity is greater in higher modes.

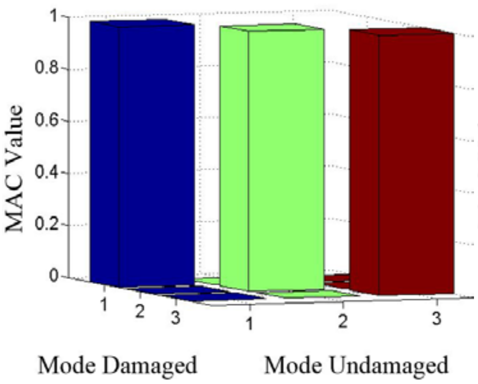

a) Theoretical

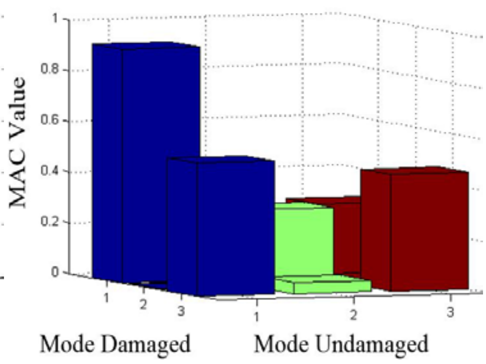

b) Experimental

Figure 8. MAC graphs of experimental specimen and theoretical model.

3.5. Damage detection by wavelet

One of the most widely used and suitable methods for detecting damage in structures is the WT method. In the present paper, the CWT was used to detect the location of the damage in the specimens. The wavelet and specially, the CWT will be discussed in the following.

3.5.1. Wavelet transform

A wavelet transform is a mathematical tool that transforms the original signal into another form to indicate the characteristic of the original signal [35, 36].

3.1.1.1. Continuous Wavelet Transform(CWT)

The wavelet transform of a signal x(t) is calculated using Eq. (4), in which, the signal is compared with a set of template functions $(\psi_{s,\tau}(t))$ obtained from the scaling (i.e., dilation and contraction) and shifting (i.e., translation along the time axis) of a base wavelet $\psi(t)$ and looking for their similarities.

The base wavelet is a small wave that has an oscillating wavelike characteristic and has its energy concentrated in time [35, 36].

$$\psi_{s,\tau}(t) = \frac{1}{\sqrt{s}} \psi\left(\frac{t-\tau}{s}\right) \quad (3)$$

$$wt(s,\tau) = \langle x(t), \psi_{s,\tau} \rangle = \frac{1}{\sqrt{s}} \int_{-\infty}^{+\infty} x(t) \psi^{*}\left(\frac{t-\tau}{s}\right) dt \quad (2)$$

Where the symbol $s > 0$ represents the scaling parameter, which determines the time and frequency resolutions of the scaled base wavelet $\psi(t-(\tau/s))$. The specific values of s are inversely proportional to the frequency. The symbol τ is the shifting parameter, which translates the scaled wavelet along the time axis. The symbol * denotes the complex conjugation of the base wavelet $\psi(t)$ [35-37].

As the wavelet contains two parameters, transforming a signal with the wavelet basis means that such a signal will be projected into a 2D, time-scale plane. Because of the localization feature of the violin, the wavelet transform is obtained from its time characteristics.

Wavelet deubechies (db) was used for damage localization in this study. According to Figure 9, the damage location is carefully and accurately determined. As shown in Figure 9, in all the three modes of theoretical (Figures 9a-c) and laboratory (Figures 9d-9f), in the damage location which is in the center of the column, a jump is made; where the starting point and the ending point of the jump, shows the first and end of the damage which is highlighted in the Figure 9.

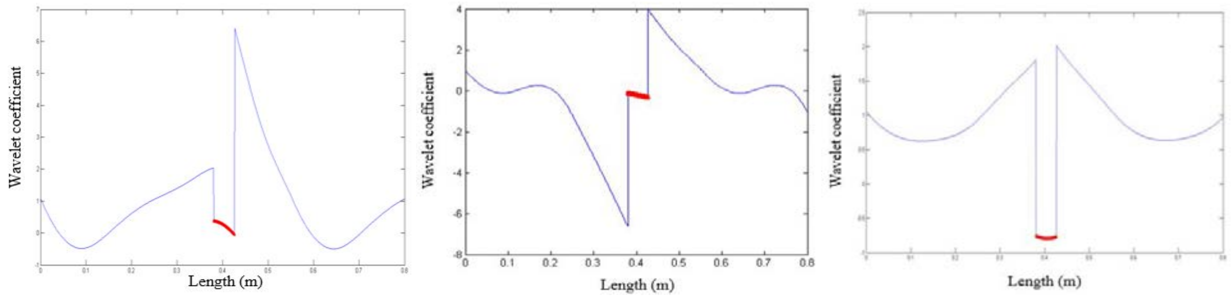

a) Model(Exp.) **b) ModelI(Exp.)** **c) ModelII(Exp.)**

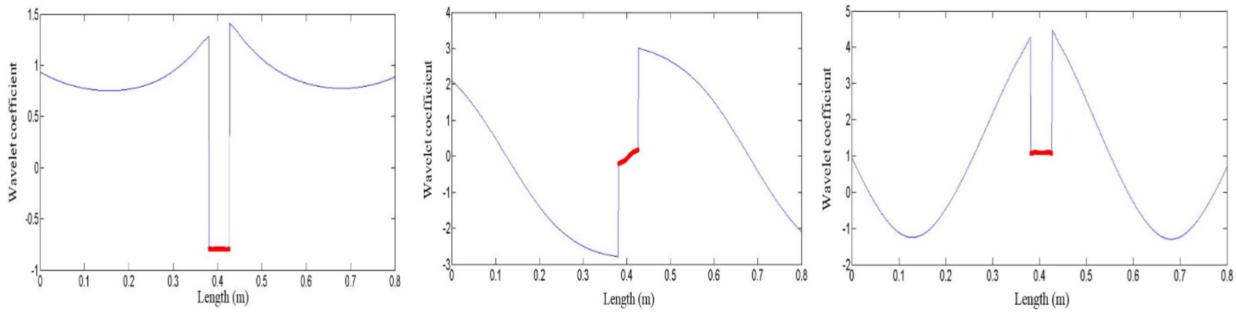

d) Model(Theo.) **e) ModelI(Theo.)** **f) ModelII(Theo.)**

Figure 9. Wavelet transform of specimens and models.

4. Conclusion

Frequency analysis, mode shape, and MAC and COMAC criteria were used in the present study to detect the presence of damage. The results of the analysis indicate that the above parameters have changed and confirm the presence of damage in the structure. Additionally, a CWT method was used to determine damage location, and a db wavelet was used to investigate it which could well detect the location of damage. The above studies have been performed in both theoretical and laboratory conditions. In laboratory mode, a

Coherence parameter has been determined to confirm the accuracy of the test, which indicates the high accuracy of the tests performed and the accuracy of the data.

5. Acknowledgements

The tests of the present study were carried out in the Vibration Laboratory of the ITRAC Company. Hereby, Mr. K. B. Abadi and Mr. Khatami who have worked hard and helped researchers in performing the tests, are sincerely appreciated.

References

1. Salawu, O.S. Williams, C. Bridge assessment using forced-vibration testing. Journal of structural engineering. 1995. Vol. 121. No. 2. Pp. 161–173.
2. Salawn, O.S. Damage location using vibration mode shapes. Proceedings of 12th IMAC. 1994. Pp. 933–938.
3. Salawu, O.S. Detection of structural damage through changes in frequency: a review. Engineering structures. 1997. Vol. 19. No. 9. Pp. 718–723.
4. Lyapin, A., Shatilov, Y. Vibration-based Damage Detection of the Reinforced Concrete Column. Procedia Engineering. 2016. Vol. 150. Pp. 1867–1871.
5. Yang, C., Oyadiji, S.O. Damage detection using modal frequency curve and squared residual wavelet coefficients-based damage indicator. Mechanical Systems and Signal Processing. 2017. Vol. 83. Pp. 385–405.
6. Wang, J.T.S., Liu, Y.Y., Gibby, J.A. Vibrations of split beams. Journal of Sound Vibration. 1982. Vol. 84. Pp. 491–502.
7. Narkis, Y. Identification of crack location in vibrating simply supported beams. Journal of sound and vibration. 1994. Vol. 172. No. 4. Pp. 549–558.
8. Messina, A., Jones, I.A., Williams, E.J. Damage detection and localization using natural frequency changes. Proceedings of conference on Identification in Engineering Systems. 1996. Pp. 67–76.
9. Messina, A., Williams, E.J., Contursi, T. Structural damage detection by a sensitivity and statistical-based method. Journal of sound and vibration. 1998. Vol. 216. No. 5. Pp. 791–808.
10. Gadelrab, R.M. The effect of delamination on the natural frequencies of a laminated composite beam. Journal of Sound and Vibration. 1996. Vol. 197. No. 3. Pp. 283–292.
11. Kessler, S.S., et al. Damage detection in composite materials using frequency response methods. Composites Part B: Engineering. 2002. Vol. 33. No. 1. Pp. 87–95.
12. Della, C.N., Shu, D. Vibration of delaminated composite laminates: A review. Applied Mechanics Reviews. 2007. Vol. 60. No. 1. Pp. 1–20.
13. Alnefaie, K. Finite element modeling of composite plates with internal delamination. Composite Structures. 2009. Vol. 90. No. 1. Pp. 21–27.
14. Salawu, O.S. Detection of structural damage through changes in frequency: a review. Engineering structures. 1997. Vol. 19. No. 9. Pp. 718–723.
15. Fan, W., Qiao, P. Vibration–based damage identification methods: a review and comparative study. Structural health monitoring. 2011. Vol. 10. No. 1. Pp. 83–111.
16. Kim, J.T., Ryu, Y.S., Cho, H.M., Stubbs, N. Damage identification in beam–type structures: frequency–based method vs mode-shape-based method. Engineering structures. 2003. Vol. 25. No. 1. Pp. 57–67.
17. Wei, Z. Yam, L.H. Cheng, L. Detection of internal delamination in multi–layer composites using wavelet packets combined with modal parameter analysis. Composite Structures. 2004. Vol. 64. No. 3–4. Pp. 377–387.
18. Hong, J.-C., et al. Damage detection using the Lipschitz exponent estimated by the wavelet transform: applications to vibration modes of a beam. International journal of solids and structures. 2002. Vol. 39. No. 7. Pp. 1803–1816.
19. Katunin, A. Damage identification in composite plates using two–dimensional B–spline wavelets. Mechanical Systems and Signal Processing. 2011. Vol. 25. No. 8. Pp. 3153–3167.
20. Chang, C.-C., Chen, L.-W. Detection of the location and size of cracks in the multiple cracked beam by spatial wavelet based approach. Mechanical Systems and Signal Processing. 2005. Vol. 19. No. 1. Pp. 139–155.
21. Petinov, S.V., Guchinsky, R.V., Sidorenko, V.G. Damage identity in fatigue assessment of structures. Magazine of Civil Engineering. 2016. 61(1). Pp. 82–88. DOI: 10.5862/MCE.61.8
22. Benin A.V., Semenov A.S., Semenov S.G., Beliaev M.O., Modestov V.S. Methods of identification of concrete elastic–plastic–damage models. Magazine of Civil Engineering. 2017. 77(8). Pp. 279–297. DOI: 10.18720/MCE.76.24
23. Wang, Q.-T., Chang, X. Analysis of concrete–filled steel tubular columns with. Steel and Composite Structures. 2013. Vol. 15. No. 1. Pp. 41–55.
24. Rezaifar, O., Yoonesi, A., Yousefi, S. H., Gholhaki, M. Analytical study of concrete–filled effect on the seismic behavior of restrained beam–column steel joints. Scientia Iranica. Transaction A, Civil Engineering. 2016. Vol. 23. No. 2. Pp. 475.
25. Rezaifar, O. Younesi, A. Finite element study the seismic behavior of connection to replace the continuity plates in (NFT/CFT) steel columns. Steel and Composite Structures. 2016. Vol. 21. No. 1. Pp. 73–91.
26. Rezaifar, O., Nazari, M. Experimental Study the Seismic Behavior of Types of Continuity Plates in Beam–to–HSS Column Connections, 2016. MSc. Thesis, Semnan university, Semnan, Iran.
27. Rezaifar, O., Monavari, M. Experimental Study the Seismic Behavior of Types of Continuity Plates in Beam–to–CFT Column Connections, 2016. MSc. Thesis, Semnan university, Semnan, Iran.
28. Rezaifar, O, Younesi, A. Experimental study discussion of the seismic behavior on new types of internal/external stiffeners in rigid beam–to–CFST/HSS column connections. Construction and Building Materials. 2017. Vol. 136. Pp. 574–589.
29. XU, B., Li, B., Song, G. Active debonding detection for large rectangular CFSTs based on wavelet packet energy spectrum with piezoceramics. Journal of Structural Engineering. 2012. Vol. 139. No. 9. Pp. 1435–1443.
30. Xu, B., Zhang, T., Song, G., Gu, H. Active interface debonding detection of a concrete–filled steel tube with piezoelectric technologies using wavelet packet analysis. Mechanical Systems and Signal Processing. 2013. Vol. 36(1). Pp. 7–17.

31. Ri, H., Ni, B. Embedded Interface Debonding Detection for an Irregular Complex Multi–chamber Steel Reinforced Concrete Column with PZT Impedance. Structural Health Monitoring. 2015.
32. Pandey, A.K., Biswas, M., Samman, M.M. Damage detection from changes in curvature mode shapes. Journal of sound and vibration. 1991. Vol. 145. No. 2. Pp. 321–332.
33. Duan, W.H., Wang, Q., Quek, S.T. Applications of piezoelectric materials in structural health monitoring and repair. Selected research examples. Materials. 2010. Vol. 3. No. 12. Pp. 5169–5194.
34. Frswell, M., Mottershead, J.E. Finite element model updating in structural dynamics. Springer Science & Business Media. 2013.
35. Gao, R.X., Yan, R. Wavelets: Theory and applications for manufacturing. Springer Science & Business Media. 2010.
36. Debnath, L., Shah, F.A. Wavelet transforms and their applications. Boston: Birkhäuser, 2002.
37. Stephane, M. A wavelet tour of signal processing: the sparse way. Academic press. 2008.

Contacts:

Adel Younesi: +989113242951; a.younesi@semnan.ac.ir

Omid Rezaifar: +982333383761; orezayfar@semnan.ac.ir*

Majid Gholhaki: +982333654121; mghlhaki@semnan.ac.ir

Akbar Esfandiari: +982164545041; a_Esfandiari@aut.ac.ir